# Improved Thermal-Vacuum Compatible Flat Plate Radiometric Source For System-Level Testing Of Optical Sensors

Mark A. Schwarz[a], Craig J. Kent[a], Robert Bousquet[b], Steven W. Brown[c]

[a]Stellar Solutions Inc., Palo Alto, CA, USA 94306, [b]Genesis Engineering Solutions Inc, Lanham, MD, USA 20706,
[c]National Institute of Standards and Technology, Gaithersburg, MD, USA 20899

## ABSTRACT

This work describes the development of an improved vacuum compatible flat plate radiometric source used for characterizing and calibrating remote optical sensors, in situ, throughout their testing period. The original flat plate radiometric source was developed for use by the VIIRS instrument during the NPOESS Preparatory Project (NPP). Following this effort, the FPI has had significant upgrades in order to improve both the radiometric throughput and uniformity. Results of the VIIRS testing with the reconfigured FPI are reported and discussed.
Keywords: Calibration, radiometry, remote sensing, source.

## 1. INTRODUCTION

Satellite-based sensors typically require sources that can travel with the sensor through all phases of testing, ensuring the quality and trending any changes in the sensor that may have occurred post-test. The Flat Plate Illuminator (FPI) program developed a vacuum-compatible radiometric source that could be used during the Sensor- and the Spacecraft-level testing of the Visible Infrared Imager Radiometer Suite (VIIRS) Sensor as a quality control check for the instrument's radiometric stability.[1] The first version of the FPI was used during the National Polar orbiting Operational Environmental Satellite System (NPOESS) Preparatory Project (NPP) at the Spacecraft-level for radiometric performance trending of the NPP VIIRS Flight 1 Sensor baseline acceptance testing and Spacecraft thermal vacuum (TVAC) testing.[2] After this testing period, areas of improvement in the source were identified and incorporated into an upgraded version of the FPI which was developed and tested. These improvements extended from the NPP FPI[1] to the next-generation JPSS FPI from 2010 through 2014[8]. The improved version of the FPI is currently being utilized for the Joint Polar Satellite System (JPSS), which is the next-generation low earth orbit (LEO) suite of operational environmental satellites. These satellites will circle the Earth approximately once every 100 minutes, providing timely global information about the atmosphere, oceans, land, and near-space environment.[1,2]

## 2. GENERAL JPSS FPI DESCRIPTION

In general, the JPSS FPI consists of five independent, separable components: sources with supporting electronics, a set of optical fiber bundles, the flat plate illuminator itself, the monitor/external detector(s), and, finally, the computer control/software. All of these components have been designed to be transported to a Sensor's test site. The JPSS FPI is equipped with three 300 W compact Xe arc sources[5] and one supercontinuum[6] (S/C) laser-based source from NKT Photonics.

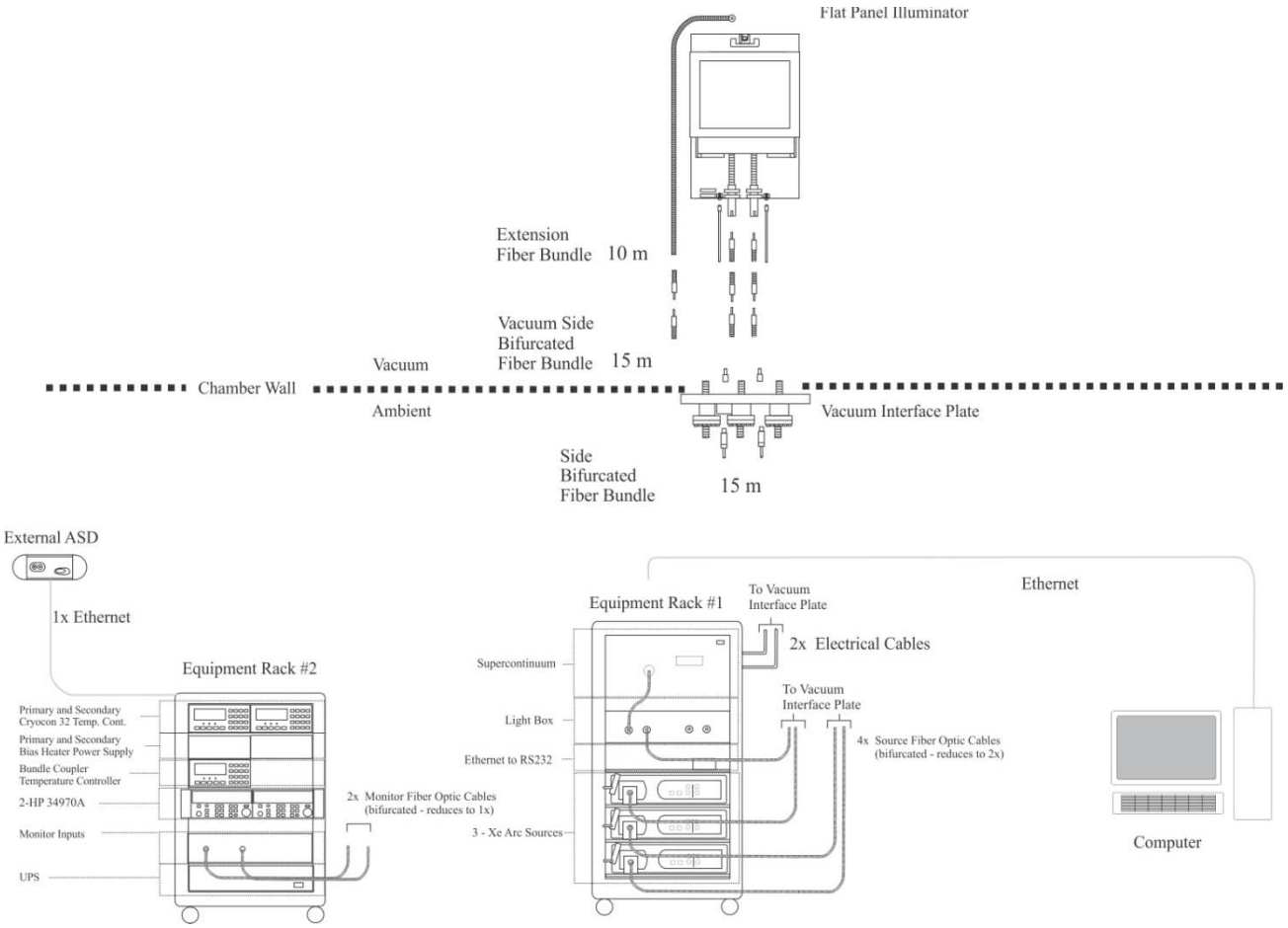


**Figure 1: JPSS FPI schematic.**

The Xe arc sources consist of the Xe arc lamp, a 3 mm quartz integrating rod, a variable shutter assembly and a fiber interface/adapter for repeatability when connecting a fiber bundle to the source. The Xe arcs are used as the primary source of radiance for the M1 and M2 bands and as a supplement for the radiance in the remaining bands. The shutter sits in between the lamp and the quartz integrating rod and is used to control the amount of source flux coupled into the fiber bundle. The source integrating rods have been decreased from the typical 6 mm to 3 mm, resulting in a numerical aperture (NA) of approximately 0.5. Each of the three Xe arc sources supplies one of the legs of the bifurcated source fiber bundles. A set of fans has also been added to the Xe arc sources to regulate the temperature of the source-fiber bundle interface.

A single S/C source is used to provide additional radiance in all of the bands above M1 and M2. The S/C source is operated at a constant output flux and a custom attenuator/coupling box is used to vary the S/C flux into the remaining leg of a bifurcated source fiber bundles. The attenuator box consists of a powered mirror assembly which is used to both reduce the irradiance on a variable (neutral density) attenuator and more efficiently couple the S/C output flux into the FPI fiber bundle.

The shutters and variable attenuator are used in conjunction with the computer control to create a series of radiance levels during the testing. These levels are tuned/measured beforehand using both the external/monitor spectroradiometer, with each source varied to produce a percentage of the band-averaged

radiance. These levels are reproduced during the Sensor test period for instrument gain trending during the test period.

These sources are housed in a rack-mounted (Rack 1) shipping container, while a second rack-mount (Rack 2) container holds the heater power supplies, the data acquisition and control hardware, and the communications interfaces (Figure 2). In Rack 2, there are two Cryo-Con temperature controllers (CC1 and CC2) which serve as the primary means for the FPI's temperature control and two Hewlett Packard (HP) 50-W DC heater power supplies (PS1 and PS2), used to provide bias heating when needed. Each of the bias power supplies is capable of maintaining the FPI temperature at +35°C in a liquid nitrogen shroud environment used during testing. An additional temperature controller is used to regulate the temperature of the fiber extension bundle coupler. An Agilent 34970A data acquisition system is used to log the data from both the filter radiometers and thermistors. A monitor spectroradiometer and silicon detector are also housed in Rack 2, providing radiance information while the FPI is be used as a test source. An external spectroradiometer, that is maintained under calibration, is used to transfer a calibration to the monitor spectroradiometer before and after any sensor testing. All control and data logging communication to the racks/external spectroradiometer is accomplished with a PC computer via Ethernet connection, providing flexibility in the equipment and control computer locations.

**Figure 2. JPSS FPI racks with sources, control electronics, and communications. Rack 1 is on the left; Rack 2 on the right.**

A total of six sets of fiber bundles are used with the FPI: three bifurcated (30 m) and three single fiber bundles (10 m). The bifurcated fiber bundles contain a vacuum feed-through interface which uses a conflate seal for the vacuum interface. The other half of the fiber flange interfaces sit on a larger o-ring sealed flange that is

used as the vacuum interface in the TVAC test vacuum chamber. Two of these (the source bundles) are used to transfer the source flux from the Xe arc and S/C sources to the FPI while the remaining (the monitor bundle) has the single ferrule side-mounted above the flat plate. The monitor bundle is used to collect the radiance from the flat plate and couple it to both a spectroradiometer and a silicon detector. The three shorter 10 m fiber bundles serve as extensions to the bifurcated fiber bundles, facilitating the integration of the FPI into the test vacuum chamber. These fiber bundles directly (i.e. butted end to end) couple to the bifurcated bundles via a heated bundle coupler inside the vacuum chamber. The temperature of this coupler is regulated to minimize any thermal effects that might cause radiance variations during TVAC testing.

In addition to the monitor fiber bundle, three Gershun-tube filter radiometers (FRs) monitor the spectral radiance from three of the four corners of the FPI, all of which lie outside of the VIIRS FOV (see Figure 3). The filter radiometers are silicon detector elements, one of which is unfiltered. Of the remaining two, one has a 10 nm Full Width Half Maximum (FWHM) bandpass filter centered at 410 nm, and the other has a 10 nm FWHM bandpass filter centered at 860 nm. The filter radiometers are located above and to the top and bottom of the flat plate; they view the radiance emitted from the flat plate at approximately 45° from normal. The silicon detectors are coupled to the FPI wiring harness through BNC-terminated coax cables.

There are two types electrical harnesses; one is used to relay the heater current/thermistor voltage and the other is used to collect the filter radiometer signals from the FPI. Both types of harnesses have ambient, vacuum, and extension sections. The extension section (similar to the fiber extensions) facilitates the integration of the FPI into the vacuum chamber. Additionally, a transimpedance amplifier sits on the FPI vacuum flange and relays the detector signal from the extension/vacuum electrical cable to the equipment racks through the ambient electrical cable.

The dimension of the FPI is approximately 66 cm by 41 cm by 14 cm (not including the standoffs). The FPI radiating surface is approximately 25 cm by 35 cm. An ambient test fixture has been constructed to allow the FPI to be positioned in a manner similar to the vacuum test fixture which is used during the TVAC testing.

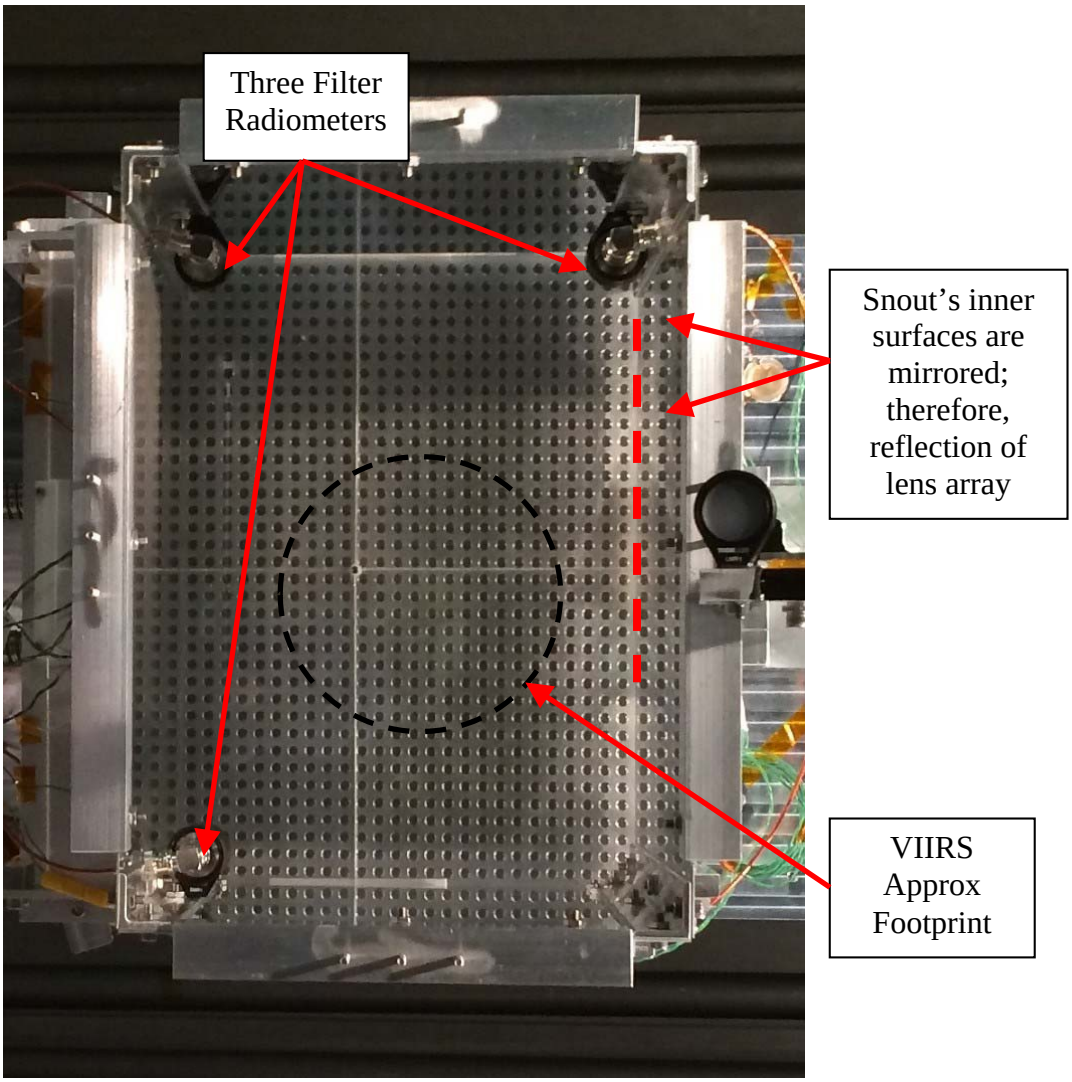


**Figure 3. Front view of JPSS FPI showing the three filter radiometers inside the FPI snout. The ground glass diffuser was removed from the front of the snout in order to view the inside.**

## 3. FPI IMPROVEMENTS AND JPSS FPI RADIOMETRIC PERFORMANCE IN AMBIENT ENVIRONMENT AT SENSOR-LEVEL

The improved FPI was intended to address the three shortcomings that had been identified in the NPP FPI[8]. These shortcomings were identified as the following:

1. Excessive non-uniformity, both spatial and angular.
2. Low throughput.
3. Low radiometric stability and repeatability measurement-to-measurement.

To address these issues, several areas of the FPI had been identified for upgrades: the flat plate, the fiber coupling at the FPI, and indexing the optical coupling joints of the FPI.

The first two parameters, non-uniformity and low throughput, were addressed by incorporating an engineered diffuser plate and lenslet array in front of the fiber plate[8]. The third performance parameter that was addressed in the JPSS FPI was the radiometric stability and repeatability from measurement to measurement, as well as from assembly to disassembly to reassembly. Improved mechanical fixturing and mounting techniques were retrofitted to all accessible optical interfaces to facilitate repeatable connection orientations. An indexing system was created and adhered to in order to ensure the correct orientation of the optical connectors and fasteners are used while not allowing them to rotate in their mounts after inserted. Moreover, the addition of integrating rods to the FPI fiber couplers reduced the source radiances dependence on the orientation of the fiber bundles at this point.

The FPI was completely assembled, disassembled, and reassembled and test measurements were conducted to demonstrate instrument repeatability a total of three times before the unit needed to be packaged and shipped to Goddard Space Flight Center (GSFC) for FPI TVAC testing. The radiometric performance from build-to-build did not vary more than ±5% overall, which has been deemed acceptable for VIIRS testing. This is particularly important since the FPI has be tested, disassembled, and shipped to different locations.

The final configuration was first shipped to GSFC to verify the FPI's performance under TVAC conditions and then directly shipped to El Segundo, CA, to support VIIRS Sensor-level testing.

The Sensor-level testing in El Segundo, CA, was carried out by, first, aligning the FPI with the VIIRS Sensor and producing a set of radiance levels (agreed upon beforehand) by varying the output of the sources. Pre- and post-measurements of the FPI's radiance were carried out by measuring the source radiance with an external ASD spectroradiometer (PANalytical). All testing was performed in the optical configuration that will be used at TVAC testing (i.e. extension fibers, etc.) for the JPSS Spacecraft.

Figure 4, below, depicts the spectral radiance levels used in the Ambient Sensor-level testing.

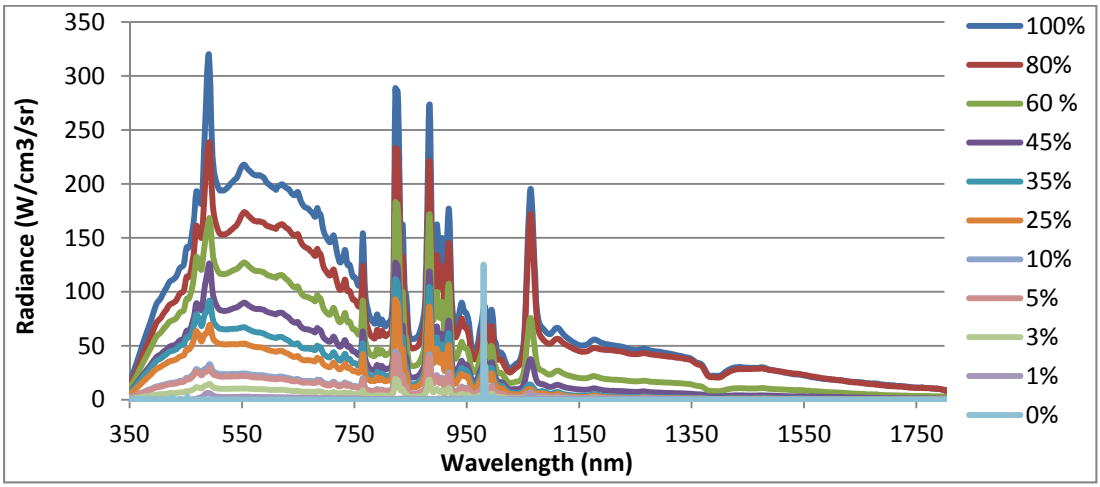


**Figure 4: Spectral radiance levels used during VIIRS Ambient Sensor-level testing.**

In Table 1, it can be seen that the JPSS FPI radiance, incorporating the upgrades and without the glass diffuser (3rd column), exceeds the requirements for each of the VIIRS bands (2nd column) in all of the bands, confirming that the JPSS FPI's throughput was appreciably increased. The radiance in M1 definitely suffers appreciable losses due to absorption in that waveband from the BK7 lenses and the BK7 engineered diffuser.

This was also due to the fact that the engineered diffuser was optimized near the center of the visible waveband.

**Table 1: Measured band-averaged radiance at Ambient Sensor-level testing, compared to minimum required radiance.**

| | Min Req Radiance | FPI Source Levels | | | | | | | | | | |
|---|---|---|---|---|---|---|---|---|---|---|---|---|
| | At 100% | 100% | 80% | 60% | 45% | 35% | 25% | 15% | 10% | 5% | 3% | 0% |
| M1 | 60 | 100.11 | 80.67 | 66.25 | 44.95 | 40.68 | 32.58 | 14.00 | 13.00 | 5.37 | 0.00 | 0.00 |
| M2 | 52 | 119.26 | 96.16 | 78.99 | 53.90 | 48.78 | 39.19 | 17.06 | 15.85 | 6.65 | 0.03 | 0.18 |
| M3 | 44 | 252.54 | 196.67 | 144.55 | 105.54 | 78.85 | 60.34 | 28.40 | 25.28 | 12.64 | 4.85 | 0.26 |
| M4 | 24 | 191.13 | 152.20 | 111.41 | 78.65 | 58.98 | 45.79 | 21.41 | 19.37 | 9.19 | 2.45 | 0.12 |
| M5 | 17.2 | 167.68 | 132.30 | 90.11 | 61.72 | 45.16 | 34.90 | 16.64 | 15.14 | 7.04 | 1.66 | 0.09 |
| M6 | 10.6 | 134.29 | 107.34 | 75.57 | 51.75 | 38.79 | 30.21 | 14.50 | 13.25 | 6.14 | 1.31 | 0.08 |
| M7 | 6.8 | 115.94 | 96.01 | 69.21 | 46.93 | 37.82 | 30.69 | 14.94 | 13.75 | 6.59 | 0.91 | 0.06 |
| M8 | 7 | 41.16 | 37.47 | 15.21 | 6.54 | 2.21 | 1.48 | 1.04 | 0.82 | 0.53 | 0.62 | 0.02 |
| M9 | 1.2 | 21.88 | 20.83 | 8.11 | 3.18 | 1.10 | 0.73 | 0.56 | 0.45 | 0.23 | 0.34 | 0.02 |
| M10 | 2.4 | 14.54 | 14.59 | 5.32 | 1.97 | 0.63 | 0.42 | 0.33 | 0.24 | 0.12 | 0.25 | 0.03 |

The uniformity was also measured in ambient conditions by VIIRS and is shown in Figure 5. The non-uniformity shown in the figure exhibits better than ±5% within ±3°. The requirement for the JPSS FPI is <±10% within ±2°, which means the JPSS FPI meets the requirement in ambient conditions.

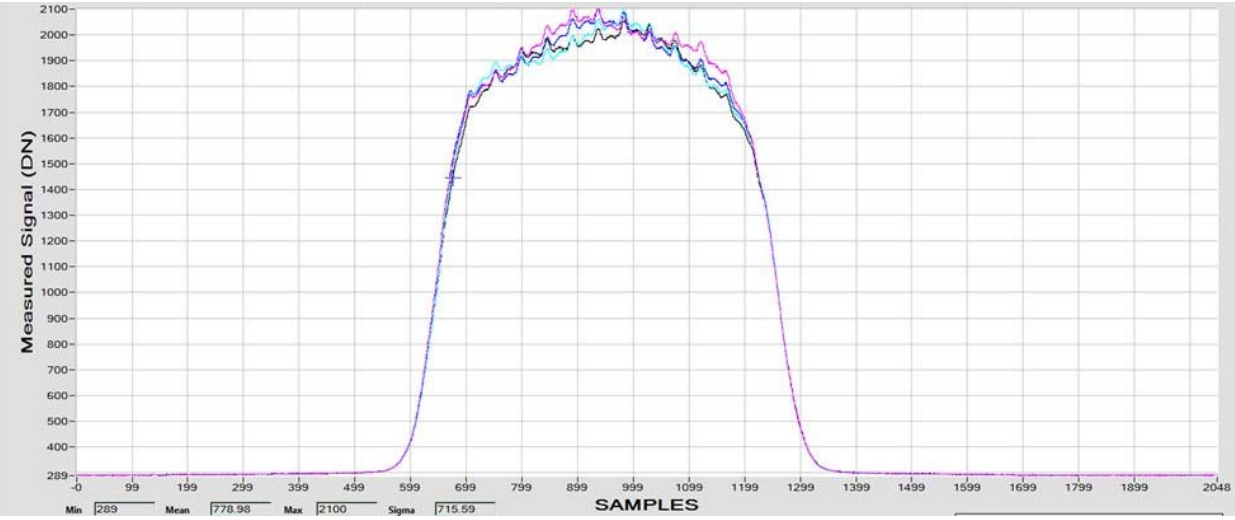


**Figure 5: Uniformity of JPSS FPI measured by VIIRS Band M1.**

However, note the periodic structure (peaks) across the central lobe in the figure. The periodic peaks are due to the newly-introduced engineered diffuser and also removing the ground-glass diffuser from the end of the snout. These peaks were deemed to be unacceptable for sensor gain trending and signal-to-noise trending. It was, therefore, agreed at the Sensor-level that this would be addressed by re-introducing the ground-glass diffuser on the end of the snout, provided that there is enough radiance to still produce acceptable radiance levels to the VIIRS Sensor. Unfortunately, we did not have time to re-install the glass diffuser and measure with the VIIRS Sensor by the time our testing window closed at the end of 2014.

After the Sensor-level Ambient test campaign, it was determined that two additional factors would help the FPI to meet the performance goals of the FPI/VIIRS measurements during subsequent Spacecraft-level Ambient and TVAC testing. This included the additional improvement of the spatial uniformity, due to the small amount of residual structure that remained at the VIIRS image plane, which in turn would facilitate the ability of the VIIRS Team to evaluate the Sensor noise level. Additional configuration changes were made at this time, including:

- Incorporating the ground-glass diffuser back into the measurements
- Replacing the Xe arc source lamps
- Utilizing a spare fiber bundle (which had been determined to provide increased throughput). One of the vacuum fiber bundles was found to have a significant amount of internal damage, so was replaced with the spare bundle.

The Sensor-level Ambient test campaign concluded at this juncture. The FPI Team disassembled, packaged, and shipped the FPI to the Spacecraft Integrator facility, in preparation for Spacecraft-level Ambient and TVAC testing.

## 4. JPSS FPI RADIOMETRIC PERFORMANCE IN AMBIENT ENVIRONMENT AT SPACECRAFT-LEVEL

After the VIIRS Sensor had been integrated onto the Spacecraft mechanical bus, the Spacecraft-level test campaign was carried out with the FPI to ensure Sensor quality and for continued trending. In addition to the changes mentioned in the previous section, the radiance levels had been re-tuned for better spectral conformity to the percentage levels. The FPI spectral radiance levels used in this test are shown in Figure 6. These data were taken before Spacecraft-level Ambient testing commenced.

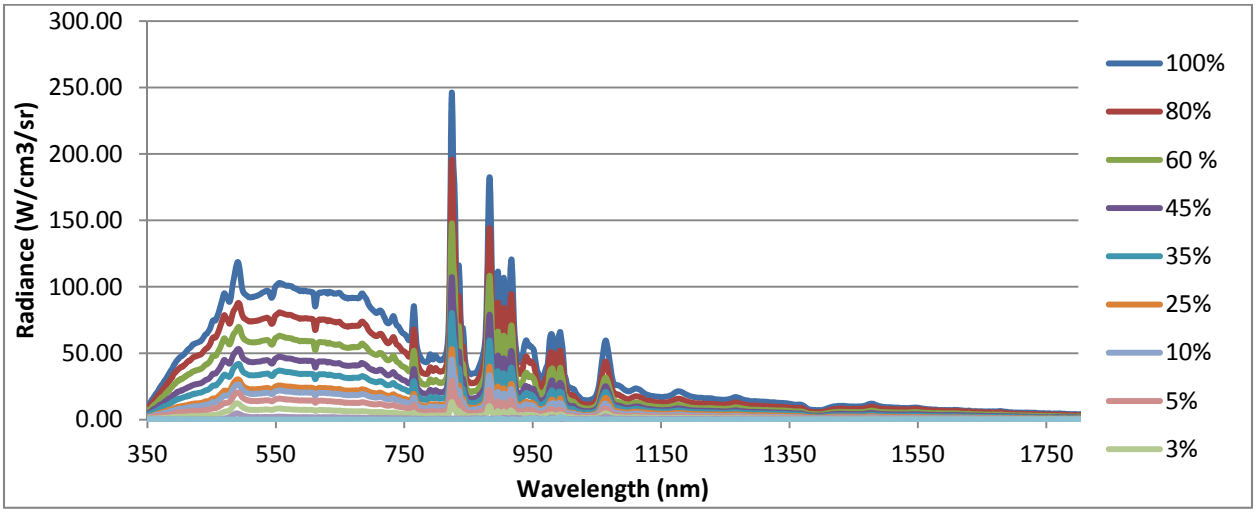


Figure 6: FPI spectral radiance levels used for Spacecraft-level Ambient testing.

The band-averaged radiance values, prior to Spacecraft-level Ambient testing, for bands M1 to M10 are listed in Table 2. It can be seen that the radiance for M1 (52.04) is slightly below the required level (60), but this more than what was produced for the NPP Spacecraft, so was deemed to be acceptable to proceed. All remaining bands received ample radiance from the JPSS FPI. The primary reason the radiance levels are noticeably reduced from what was produced at the Sensor-level testing (Table 1) is that the ground-glass diffuser was re-installed onto the snout of the FPI to address the periodic peaks exhibited in Figure 5.

**Table 2: Band-averaged spectral radiance levels (11 Levels) prior to Spacecraft-level Ambient testing, for Bands M1 to M10, using the ground-glass diffuser at BATC.**

| | Min Req Radiance | FPI Source Levels | | | | | | | | | | |
|---|---|---|---|---|---|---|---|---|---|---|---|---|
| | At 100% | 100% | 80% | 60% | 45% | 35% | 25% | 15% | 10% | 5% | 3% | 0% |
| M1 | 60 | 52.04 | 43.15 | 33.43 | 24.02 | 17.71 | 10.95 | 8.98 | 5.88 | 2.38 | 0.02 | 0.01 |
| M2 | 52 | 67.62 | 56.03 | 43.48 | 31.34 | 23.22 | 14.38 | 11.83 | 7.71 | 3.17 | 0.04 | 0.00 |
| M3 | 44 | 105.87 | 81.80 | 64.68 | 49.16 | 38.58 | 27.39 | 23.69 | 17.89 | 10.43 | 3.67 | -0.02 |
| M4 | 24 | 100.61 | 78.81 | 61.62 | 46.23 | 35.99 | 25.06 | 21.35 | 15.39 | 8.13 | 2.16 | 0.00 |
| M5 | 17.2 | 91.69 | 70.73 | 54.64 | 40.83 | 31.53 | 21.98 | 18.55 | 12.67 | 6.25 | 1.44 | -0.02 |
| M6 | 10.6 | 74.80 | 59.17 | 45.79 | 34.26 | 26.45 | 18.38 | 15.54 | 10.65 | 5.23 | 1.16 | 0.02 |
| M7 | 6.8 | 60.83 | 48.34 | 36.66 | 27.00 | 20.60 | 14.16 | 11.93 | 7.81 | 3.75 | 0.72 | 0.06 |
| M8 | 7 | 15.22 | 11.46 | 8.32 | 6.36 | 5.23 | 3.82 | 2.69 | 1.85 | 0.99 | 0.41 | 0.01 |
| M9 | 1.2 | 8.78 | 6.83 | 4.95 | 3.72 | 2.94 | 2.04 | 1.41 | 0.91 | 0.48 | 0.21 | 0.07 |
| M10 | 2.4 | 7.01 | 6.40 | 4.58 | 3.38 | 2.50 | 1.60 | 1.11 | 0.67 | 0.48 | 0.13 | 0.04 |

The JPSS FPI's spectral radiance levels were re-measured following the Spacecraft-level Ambient test campaign and are shown in Figure 7.

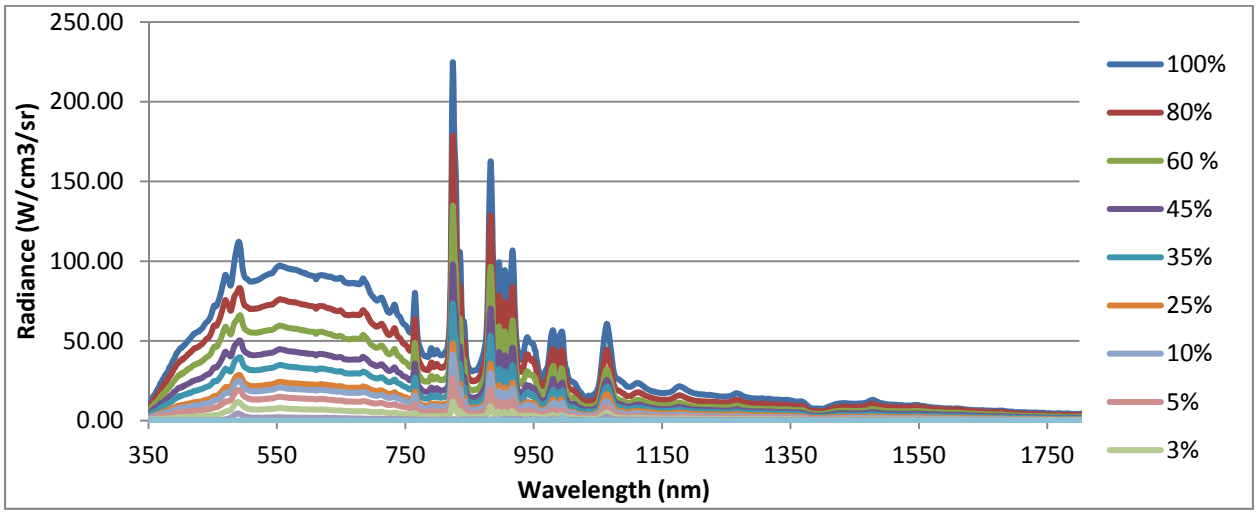


**Figure 7: JPSS FPI spectral radiance levels measured after Spacecraft-level Ambient testing.**

The band-averaged radiance values, following Spacecraft-level Ambient testing, for bands M1 to M10 are listed in Table 3, below. The radiance levels repeated, pre- to post-Ambient testing, to within ±5%, meeting our requirement for repeatability.

**Table 3: Band-averaged spectral radiance levels (11 Levels) after Spacecraft-level Ambient testing, for Bands M1 to M10, using the ground-glass diffuser at BATC.**

| | Min Req Radiance | FPI Source Levels | | | | | | | | | | |
|---|---|---|---|---|---|---|---|---|---|---|---|---|
| | At 100% | 100% | 80% | 60% | 45% | 35% | 25% | 15% | 10% | 5% | 3% | 0% |
| M1 | 60 | 50.28 | 41.69 | 32.30 | 23.20 | 17.11 | 10.58 | 8.67 | 5.68 | 2.30 | 0.02 | 0.01 |
| M2 | 52 | 65.17 | 54.01 | 41.91 | 30.21 | 22.38 | 13.86 | 11.40 | 7.43 | 3.06 | 0.04 | 0.00 |
| M3 | 44 | 100.58 | 77.71 | 61.45 | 46.71 | 36.65 | 26.02 | 22.51 | 16.99 | 9.91 | 3.49 | -0.02 |
| M4 | 24 | 96.13 | 75.29 | 58.88 | 44.17 | 34.39 | 23.94 | 20.40 | 14.70 | 7.76 | 2.07 | 0.00 |
| M5 | 17.2 | 86.14 | 66.44 | 51.33 | 38.35 | 29.62 | 20.65 | 17.43 | 11.91 | 5.88 | 1.36 | -0.02 |
| M6 | 10.6 | 69.84 | 55.25 | 42.75 | 31.99 | 24.70 | 17.16 | 14.51 | 9.95 | 4.89 | 1.08 | 0.02 |
| M7 | 6.8 | 54.35 | 43.19 | 32.76 | 24.12 | 18.41 | 12.66 | 10.67 | 6.98 | 3.35 | 0.64 | 0.05 |
| M8 | 7 | 15.34 | 11.54 | 8.39 | 6.40 | 5.27 | 3.85 | 2.71 | 1.87 | 1.00 | 0.42 | 0.01 |
| M9 | 1.2 | 9.27 | 7.21 | 5.22 | 3.93 | 3.10 | 2.15 | 1.48 | 0.96 | 0.51 | 0.22 | 0.08 |
| M10 | 2.4 | 7.34 | 6.71 | 4.80 | 3.54 | 2.61 | 1.68 | 1.16 | 0.70 | 0.50 | 0.14 | 0.05 |

## 5. SUMMARY AND CONCLUSIONS

In this work, we have described the results from Ambient Sensor- and Spacecraft-level testing with a new class of vacuum-compatible, externally illuminated, fiber-optically coupled, flat plate illuminator for the radiometric characterization and calibration of large aperture sensors. There are many challenges associated with providing a uniform radiance source that can be used in both ambient and vacuum conditions, and at the same time, is transportable to the test sites. The FPI provides a novel means of accomplishing this versus the alternative (i.e. reflectance plaques, integrating spheres, etc). Incorporating the engineered diffuser significantly increased the throughput of the FPI; however, the small amount of residual structure reduced the usefulness of the source for noise trending in VIIRS and, ultimately, the ground-glass diffuser was re-installed during the Ambient Spacecraft-level testing. The engineered diffuser, as well as the additional changes, helped to greatly improve the spatial uniformity across the FPI output (ground-glass diffuser) versus the NPP FPI.

The JPSS FPI represented in this work has an active area of 25 cm by 35 cm and a total depth under 20 cm. The overall footprint is less than 1 $m^2$. The compact size and fiber bundles allow this type of source to be placed and operated in confined spaces, for example, in a vacuum chamber, over a wide range of environmental temperatures. Other potential applications include, but are not limited to, providing a calibration of aircraft sensors *in situ* in the aircraft instrument bay just prior to and following a flight; also, configurations for in-flight calibration of aircraft sensors can also be envisioned. There is no limitation on the size of these sources or on the number of optical fibers terminated in the source plane. Consequently, applications related to the near-field characterization of larger aperture sensors, e.g. astronomical telescopes with meter-size primary mirrors, may also be possible.

## 6. ACKNOWLEDGEMENTS

We would like to acknowledge and thank NIST colleagues, Dr Ping-Shine Shaw and Dr Keith Lykke, for their assistance in the functional checkout of the JPSS FPI.

* Identification of commercial equipment does not imply recommendation or endorsement by Stellar Solutions or the National Institute of Standard and Technology, nor does it imply that the equipment identified is necessarily the best available for the purpose.

## REFERENCES

1. S.W. Brown, et al, "A vacuum-compatible flat plate radiometric source for system-level testing of optical sensors," Proc. SPIE 7474, Sensors, Systems, and Next-Generation Satellites XIII, 747412 (September 24, 2009)
2. R.R. Bousquet, et al, "Spacecraft level radiometric testing with the flat plate illuminator," Cal Con Technical Conference (2010)
3. J.E. Greivenkamp, "Field Guide To Geometrical Optics," SPIE Field Guides, Volume FG01 (2004)
4. RPC Photonics, http://www.rpcphotonics.com
5. Perkin Elmer XL3000 compact Xe arc source, http://optoelectronics.perkinelmer.com
6. NKT Photonics, http://www.nktphotonics.com
7. CeramOptec, http://www.ceramoptec.com
8. M.A. Schwarz, et al, "Improved Thermal-Vacuum Compatible Flat Plate Radiometric Source For System-Level Testing Of Optical Sensors," Proc. SPIE 9218-35, Earth Observing Systems XIX, (August 19, 2014)